E-proceedings of the 38th IAHR World Congress
September 1-6, 2019, Panama City, Panama
doi:10.3850/38WC092019-0706

DEVELOPMENT AND APPLICATION OF CALCULATION METHOD FOR AMOUNT OF SUSPENDED SEDIMENT ENTRAINMENT UNDER NON-EQUILIBRIUM CONDITIONS OF FLOWS AND SEDIMENT TRANSPORTS

TAKAHISA GOTOH [(1)], SHOJI FUKUOKA[(2)]

[(1,2)] Research and Development Initiative Chuo University 1, Tokyo, Japan,
e-mail goto510@tamacc.chuo-u.ac.jp

ABSTRACT

Large amounts of suspended sediments are transported by flood flows in sandy rivers. The suspended sediment concentration is generally calculated by the three-dimensional advection diffusion equation assuming that the flow and sediment transport near the bed are in equilibrium conditions. In this study, the quasi-3D flood flow and bed variation calculation model is developed by considering non-equilibrium two-phase motion of flow and sediment near beds. The developed model is applied to the experiment of local scouring around a cylinder by Fukuoka et.al. (1997). The calculation model is able to explain the bed scouring in front and side of the cylinder compared with the conventional model which the flow and sediment transport is in equilibrium conditions. It is examined that how the thickness of the bed load layer influences the estimation of flow and bed variation.

Keywords: Non-equilibrium flow and sediment movement, Quasi-3D flow analysis, Turbulent intensity, Bed load layer, Suspended sediment

1 INTRODUCTION

Large amounts of suspended sediments are transported by flood flows in sandy rivers. It is necessary to appropriately calculate suspended sediments entrainment and transportation during a flood. Shugar et. al.(2010) investigated effects of flow turbulence near beds produced by sand dunes on the sediment entrainments in sandy rivers. McLean (1994) et al. measured in detail the turbulence structures over the dunes in the experimental channels. They showed that vertical components of the turbulence increased on the stoss slope and lee of the sand dunes and it induced sediment entrainments.

In general, the flood flow and sediment transport in sandy rivers has been calculated by the two-dimensional flood flow and bed variation calculation model. The most of these models assumed the equilibrium bed load movement. And the suspended load was calculated by the two-dimensional advection diffusion equation. The vertical distribution of the suspended sediments was assumed to be in an equilibrium condition (Lane-Kalinske, 1941, etc.). The amount of sediment entrainments was estimated by using equilibrium sediment concentration near the beds.

Van Rijin (1984) evaluated equilibrium sediment concentration near the bed by the representing the relation between shear stress, saltation height and sediment concentration by a dimensionless parameter. Itakura et al. (1984) derived a vertical equation of motion of sand particles on the bed, taking into account the fluid forces caused by turbulence in the equilibrium conditions. And they evaluated the vertical velocity of the sand particle at the moment when the particle leaves from beds. The sediment entrainment was evaluated by using the vertical particle velocity. Nakagawa et al. (1986) defined suspended sediments when sand particles have transitioned from saltation motion to random motion due to turbulence, and calculated probabilistically the rate of the transition. However, those studies assumed that flow and sediment transport near the bed were in equilibrium conditions. The assumption of the equilibrium condition is not valid during a flood.

Chauchat et al. (2017) proposed the 3D calculation model which treated the flow and sediment transport as a two-phase motion. This calculation model was able to calculate the bed load and suspended load in a unified manner without the assumption of the equilibrium conditions near beds. However, it is difficult to apply this calculation model in the widespread area of rivers because this model has to perform three-dimensional calculation in consideration of interfered action between the flows and sediments.

Uchida and Fukuoka (2014) developed the quasi-3D flood flow calculation model which was the depth integrated model and was capable of calculating three-dimensional flow in a widespread area of rivers. However, their calculation model could not sufficiently evaluate the suspended sediments due to turbulence developed near the beds, although the suspended sediment concentration is calculated by a three-dimensional advection diffusion equation using the three-dimensional flow velocity.

In this study, a quasi-3D flood flow and bed variation calculation model based on the depth integrated model was developed to evaluate sediment entrainments and movements by considering non-equilibrium two-phase motion of flow and sediment near beds.

2 FLOW AND BED VARIATION CALCULATION MODEL CONSIDERING NON-EQUILIBRIUM TWO-PHASE MOTION OF FLOW AND SEDIMENT IN BED LOAD LAYER

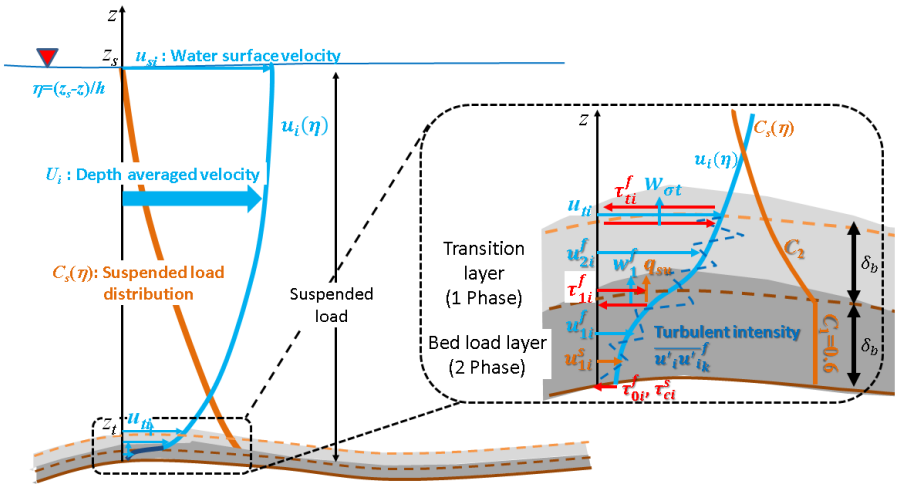

Figure 1. Definition of variables in the calculation model.

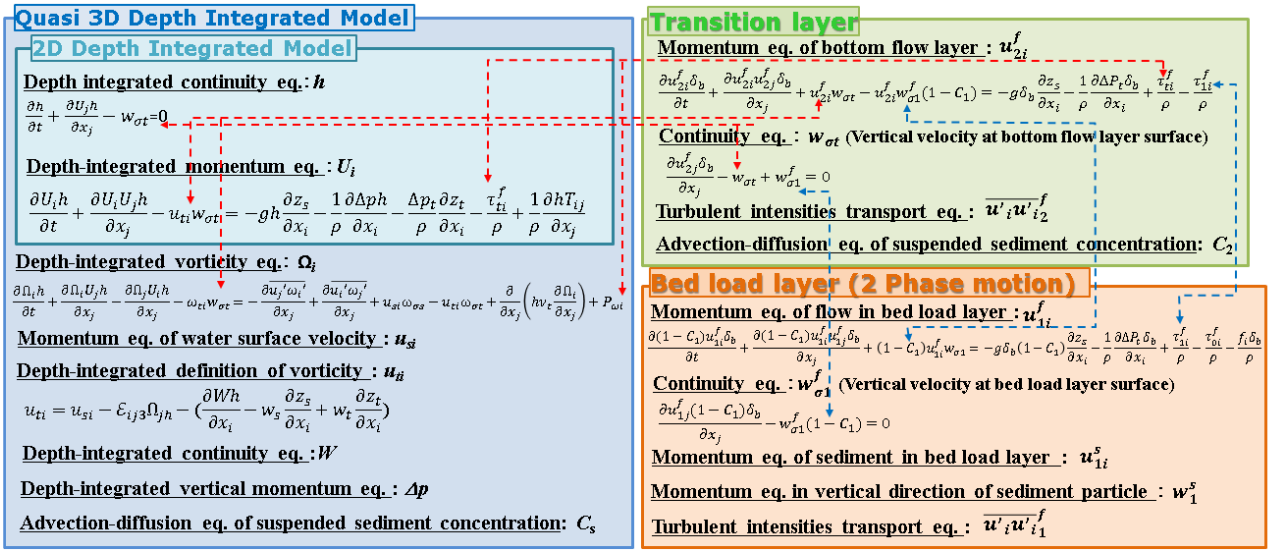

Figure 2. Frame work of the calculation model.

2.1 Framework of the calculation model.

Figure 1 shows the definition of variables in the calculation model and Figure 2 shows the framework of the calculation model. The calculation region was divided into three layers, bed load layer, transition layer and main flow layer. In bed load layer which was the lowest layer, the flow and the sediment transport were calculated by treating as the two-phase motion. The transition layer which was the second lowest region connected with the main flow and the bed load layer. And, three-dimensional flow in the main flow layer was calculated by the quasi-3D calculation model (the GBVC method, Uchida & Fukuoka, 2014). The arrows in Figure 2 indicate the exchange terms of mass and momentum of fluids and the shear stress terms acting on each layer in the equations.

The three-dimensional flows in the main flow layer and pressure distribution near the beds were calculated by applying the GBVC method. The surface velocities of the transition layer u_{ti} were evaluated by depth integrated definition of vorticity in Eq.[1], in which were calculated by the depth integrated continuity Eq.[2], the depth integrated momentum Eq.[3] and the depth integrated vorticity equations.

$$u_{ti} = u_{si} - \varepsilon_{ij3}\Omega_{jh} - \left(\frac{\partial Wh}{\partial x_i} - w_s\frac{\partial z_s}{\partial x_i} + w_t\frac{\partial z_t}{\partial x_i}\right) \quad [1]$$

$$\frac{\partial h}{\partial t} + \frac{\partial U_j h}{\partial x_j} - w_{\sigma t} = 0 \quad [2]$$

$$\frac{\partial U_i h}{\partial t} + \frac{\partial U_i U_j h}{\partial x_j} - u_{ti}w_{\sigma t} = -gh\frac{\partial z_s}{\partial x_i} - \frac{1}{\rho}\frac{\partial \Delta p h}{\partial x_i} - \frac{\Delta p_t}{\rho}\frac{\partial z_t}{\partial x_i} - \frac{\tau_{ti}^f}{\rho} + \frac{1}{\rho}\frac{\partial h T_{ij}}{\partial x_j} \quad [3]$$

$$\mathrm{T}_{ij} = -\rho\overline{u'_i u'_j} - 2\rho\nu_t S_{ij}, \quad S_{ij} = \frac{1}{2}\left(\frac{\partial U_i}{\partial x_j} + \frac{\partial U_j}{\partial x_i}\right) \quad [4]$$

Where *i,j*=1,2 (x,y direction), U_i is depth averaged flow velocity in *i* direction, h is water depth, u_{ti} is the surface velocity of the transition layer in *i* direction, u_{si} is water surface velocity in *i* direction, W is depth averaged vertical flow velocity, Ω_j is depth averaged vorticity in *j* direction, $w_{\sigma t}$ is vertical flow velocity of the transition layer, z_s is water level, z_t is surface elevation of the transition layer, Δp_t is the non-hydrostatic pressure component of the pressure at the surface of the transition layer, ν_{tt} is kinematic eddy viscosity coefficient on the surface of transition layer,ρ is density, τ_{ti}^f a is shear stresses acting on the bottom of the main flow. The shear stresses were evaluated in Eq.[5] by the vertical gradients of velocity distributions in Eq.[6].

The velocity distribution in the vertical direction of the transition layer and the bed load layer shown in Eq. [6] were determined as the third order polynomial by calculating the surface velocities of the transition layer u_{ti}, the bed load layer velocity u_{1i}^f and the transition layer velocity u_{2i}^f. And the vertical velocity distribution in the main flow was also assumed the third order polynomial in Eq.[7]. It was determined by using the mean velocity U_i, the water surface velocity u_{si}, the surface velocities of the transition layer u_{ti} and the vertical gradient of velocity at the water surface.

$$\frac{\tau_{ti}^f}{\rho} = \nu_{tt}\frac{19u_{ti} + 8u_{2i}^f - 24u_{1i}^f}{6\delta_b} \quad [5]$$

$$u_i(\eta_b) = \frac{1}{3}\left(16u_{ti} + 32u_{2i}^f - 32u_{1i}^f\right){\eta_b}^3 - \frac{1}{3}\left(16u_{ti} + 56u_{2i}^f - 40u_{1i}^f\right){\eta_b}^2 + \frac{1}{3}\left(3u_{ti} + 24u_{2i}^f - 8u_{1i}^f\right)\eta_b \quad [6]$$

$$u_i(\eta) = U_i + \Delta u_i(12\eta^3 - 12\eta^2 + 1) - \delta u_i(4\eta^3 - 3\eta^2) \quad [7]$$

Where u_i is *i* direction flow velocity of any height, $\Delta u_i = u_{si} - U_i$, $\delta u_i = u_{si} - u_{ti}$, $\eta=(z_s-z)/h$, $\eta_b=z/\delta_b$, δ_b is thickness of the bed load layer. The thickness of the bed load layer δ_b is set to α times the diameter of the bed materials. Since the thickness of the bed load layer is originally determined by the interaction between the flow and the sediment movements near the beds, it is inappropriate to make the thickness of the bed load layer constant. Therefore, the effects of the differences in the thickness of the bed load layer on the calculation results of flows and bed variations were examined in section 4.

The flow and sediment transport in the bed load layer were calculated as two phase motion. Those velocities in the bed load layer were estimated by the Reynolds-averaged continuity equations and horizontal momentum equations taking into account the interaction between flows and sediment movements. And, turbulence intensities in the horizontal and vertical directions were computed by their transport equations. The amount of sediment entrainments was evaluated by the vertical momentum equation of the sediment particles considering fluid forces caused by the Reynolds-averaged velocity and the turbulence components in the vertical direction.

The sediment transports in the transition layer and main flow layer were calculated as suspended sediments by a three-dimensional advection diffusion equation. The amount of sediment entrainments from the bed load layer was given as the bottom boundary condition of the equation. And, bed variations were calculated by the continuity equation of bed load and suspended load.

2.2 Non-equilibrium two-phase motion of flow and sediment calculation model near the bed

The equations of motion and the continuity equation of flow in the transition layer are expressed by Eq. [8] and Eq. [9], respectively. And, the equation of motion and the continuity equation of flow in the bed load layer

are also expressed by Eq. [10] and Eq. [11], respectively. Here, the horizontal shear stress term in Eq. [8] and Eq. [10] are ignored on the assumption that those layer thicknesses are thin. In addition, the non-hydrostatic pressure component of pressure Δp_t is assumed to be uniformly in the vertical direction in the transition layer and the bed load layer.

$$\frac{\partial u_{2i}^f \delta_b}{\partial t} + \frac{\partial u_{2i}^f u_{2j}^f \delta_b}{\partial x_j} + u_{2i}^f w_{\sigma t} - u_{2i}^f w_{\sigma 1}^f = -g\delta_b \frac{\partial z_s}{\partial x_i} - \frac{1}{\rho}\frac{\partial \Delta p_t \delta_b}{\partial x_i} + \frac{\tau_{ti}^f}{\rho} - \frac{\tau_{1i}^f}{\rho} \quad [8]$$

$$\frac{\partial u_{2j}^f \delta_b}{\partial x_j} - w_{\sigma t} + w_{\sigma 1}^f = 0 \quad [9]$$

$$\begin{aligned}\frac{\partial (1-C_1) u_{1i}^f \delta_b}{\partial t} + \frac{\partial (1-C_1) u_{1i}^f u_{1j}^f \delta_b}{\partial x_j} + (1-C_1) u_{1i}^f w_{\sigma 1} \\ = -g\delta_b (1-C_1)\frac{\partial z_s}{\partial x_i} - \frac{1}{\rho}\frac{\partial \Delta P_t \delta_b}{\partial x_i} + \frac{\tau_{1i}^f}{\rho} - \frac{\tau_{0i}^f}{\rho} - \frac{f_i \delta_b}{\rho}\end{aligned} \quad [10]$$

$$\frac{\partial u_{1j}^f (1-C_1)\delta_b}{\partial x_j} - w_{\sigma 1}^f (1-C_1) = 0 \quad [11]$$

Where u_{1i}^f and u_{2i}^f denotes velocities in the bed load layer and the transition layer in *i* direction, respectively. And, $w_{\sigma 1}^f$ denotes the flow velocity in the direction perpendicular to the bed load layer. The shear stress acting on the surface of the bed load layer τ_{1i}^f and the shear stress acting on the bottom of the bed load layer τ_{0i}^f are expressed by Eq. [12] and Eq. [13] using the vertical distribution of the flow velocities in the transition layer and the bed load layer expressed by Eq. [7]. ν_{t1}, ν_{t0} are kinematic eddy viscosity coefficient on the surface of bed load layer and near the bed, respectively. The sediment concentration C_1 in the bed load layer is set to a constant value of 0.6 which was around maximum value of the bed load (Van Rijin, 1984).

$$\frac{\tau_{1i}^f}{\rho} = \nu_{t1}\frac{5u_{tj} - 8u_{2i}^f + 8u_{1i}^f}{6\delta_b} \quad [12]$$

$$\frac{\tau_{0i}^f}{\rho} = \nu_{t0}\frac{3u_{tj} + 24u_{2i}^f - 8u_{1i}^f}{6\delta_b} \quad [13]$$

The horizontal particle velocity of the bed load is determined by the equation of motion shown in Eq. [14]. The hydrodynamic forces acting on the sand particles f_i are evaluated as drag forces shown in Eq. [15] and the drag coefficient is evaluated by Eq. [16] (Clift et.al, 1978). The shear stress τ_{ci}^s to which the bed load is subjected from the bottom of the bed load layer is evaluated by Eq. [17] using the dynamic friction coefficient μ_k. Here, u_{1i}^s represents the particle velocity in *i* direction of the bed load layer. R_e is Reynolds number, *d* is diameter of sediment particle, υ is kinematic viscosity coefficient. And, A_2, A_3 are a two-dimensional and three-dimensional shape factor, respectively.

$$\begin{aligned}\frac{\partial C_1 u_{1i}^s \delta_b}{\partial t} + \frac{\partial C_1 u_{1i}^s u_{1j}^s \delta_b}{\partial x_j} + C_1 u_{1i}^s w_{\sigma 1} \\ = -\frac{\rho g \delta_b}{\rho_s}\frac{\partial z_s}{\partial x_i} - \frac{1}{\rho_s}\frac{\partial \Delta P_t \delta_b}{\partial x_i} - \frac{(\rho_s - \rho) g \delta_b}{\rho_s}\frac{\partial z_b}{\partial x_i} - \frac{\tau_{ci}^s}{\rho_s} + \frac{f_i \delta_b}{\rho_s}\end{aligned} \quad [14]$$

$$\begin{aligned}f_i = \frac{1}{2}\frac{A_2}{A_3 d}\rho C_1 C_D(R_e)\left(u_{1i}^f - u_{1i}^s\right)\sqrt{\left(u_1^f - u_1^s\right)^2 + \left(v_1^f - v_1^s\right)^2 + \left(w_1^f - w_1^s\right)^2} \\ A_2 = \frac{1}{4}\pi,\ A_3 = \frac{1}{6}\pi\end{aligned} \quad [15]$$

$$C_D(R_e) = \frac{24}{R_e}(1 + 0.15{R_e}^{0.687}),\ R_e = \frac{|U_1^f| d}{\upsilon},\ |U_1^f| = \sqrt{\left(u_1^f - u_1^s\right)^2 + \left(v_1^f - v_1^s\right)^2 + \left(w_1^f - w_1^s\right)^2} \quad [16]$$

$$\tau_{ci}^s = \frac{\mu_k (\rho_s - \rho) g \delta_b u_{1i}}{|U_1|}, \qquad \mu_k = 0.4 \quad [17]$$

The bed elevation z_b can be expressed by Eq. [18] from the relationship between difference in inflow and outflow of the bed load q_{bj} and the amount of the sediment entrainment q_{su} and the sedimentation by assuming the thickness and sediment concentration in the bed load layer to be constant. Here, $q_{bj}$is bed load rate in the *j* direction. The sedimentation amount is expressed by using the falling velocity w_s of the sediment particles and the sediment concentration c_{s2} of the suspended load in the transition layer.

$$(1-\lambda)\frac{\partial z_b}{\partial t}+\frac{\partial q_{bj}}{\partial x_j}=w_s c_{s2}-q_{su},\quad q_{bj}=C_1 u_{1j}^s \delta_b \tag{18}$$

The amount of the sediment entrainment from bed per unit area and unit time is calculated by the Eq. [19] using the sediment concentration in the bed load layer and the particle velocity in the vertical direction. The vertical particle velocity is calculated from the vertical equation of motion (Eq. [20]) for the particles taking into account turbulence in the bed load layer. The flow velocity u_{1i}^f in Eq. [20] is divided into the two, the Reynolds averaged value $\bar{u}_{1i}^f$ and the turbulence components u'^f_{1i}. It is assumed that the distribution of the components of the turbulence u'^f_i follows a normal distribution, and that a flow velocity value above 25% is important for the sediment entrainment from the beds. The Eq. [20] is simplified to Eq. [21] by the assumption.

$$q_{su}=0.25C_1 w_1^s,\ \ w_1^s>0 \tag{19}$$

$$A_3(\rho_s+C_M)\rho_s \mathrm{d}^3\frac{dw_1^s}{dt}=F_z+F'_z-A_3(\rho_s-\rho)g\mathrm{d}^3=\frac{1}{2}A_2C_D\rho\mathrm{d}^2\left(\bar{w}_1^f+w'^f_1-w_1^s\right)\cdot \sqrt{\left(\bar{u}_1^f+u'^f_1-u_1^s\right)^2+\left(\bar{v}_1^f+v'^f_1-v_1^s\right)^2+\left(\bar{w}_1^f+w'^f_1-w_1^s\right)^2}-A_3(\rho_s-\rho)g\mathrm{d}^3 \tag{20}$$

$$\approx\frac{1}{2}A_2C_D\rho\mathrm{d}^2\left(\bar{w}_1^f-w_1^s+0.67\sqrt{\overline{w'w'}^f_1}\right)\cdot \sqrt{\left(\bar{u}_1^f-u_1^s\right)^2+\left(\bar{v}_1^f-v_1^s\right)^2+\left(\bar{w}_1^f-w_1^s\right)^2+0.45(\overline{u'u'}^f_1+\overline{v'v'}^f_1+\overline{w'w'}^f_1)}-A_3(\rho_s-\rho)g\mathrm{d}^3 \tag{21}$$

The suspended sediment transport is calculated by the advection diffusion equation of the sediment in the main flow layer and the transition layer in Eq. [22] and in Eq. [23].

$$\frac{\partial C_s\Delta z}{\partial t}+\frac{\partial C_s u\Delta z}{\partial x}+\frac{\partial C_s v\Delta z}{\partial y}+\frac{\partial C_s w\Delta z}{\partial z}=\frac{\partial}{\partial x}\left(\nu_t\Delta z\frac{\partial C_s}{\partial x}\right)+\frac{\partial}{\partial y}\left(\nu_t\Delta z\frac{\partial C_s}{\partial y}\right)+\frac{\partial}{\partial z}\left(\nu_t\Delta z\frac{\partial C_s}{\partial z}\right) \tag{22}$$

$$\frac{\partial C_2\delta_b}{\partial t}+\frac{\partial C_2 u_{2i}^f\delta_b}{\partial x}+\frac{\partial C_2 v_{2i}^f\delta_b}{\partial y}+C_2 w_{1i}^f =\frac{\partial}{\partial x}\left(\nu_{t2}\delta_b\frac{\partial C_2}{\partial x}\right)+\frac{\partial}{\partial y}\left(\nu_{t2}\delta_b\frac{\partial C_2}{\partial y}\right)+\frac{\partial}{\partial z}\left(\nu_{tt}\frac{\partial C_2}{\partial z}\right)\ +q_{su}-C_2w_s \tag{23}$$

The horizontal and vertical components of the turbulence intensity in the bed load layer and the transition layer are calculated by the transport equations of the turbulence intensity shown in Eq. [24]. Here, the kinetic eddy viscosity coefficients used for the calculation of the shear stresses in Eq. [12] and Eq. [13] are evaluated by the Eq. [26] using the turbulence intensity. The dissipation rate ε of the turbulence is evaluated by Eq. [26], and y_p is the dimension of length.

$$\frac{\partial\overline{u'_\iota u'_\iota}^f_k\delta_b}{\partial t}+\bar{u}_{\jmath}{}^f_k\frac{\partial\overline{u'_\iota u'_\iota}^f_k\delta_b}{\partial x_j}+2\overline{u'_\iota w'}^f_k\frac{\partial\bar{u}_\iota}{\partial z}=\nu\left(\frac{\partial^2\overline{u'_\iota u'_\iota}^f_k}{\partial {x_j}^2}\right)-C_1\frac{\varepsilon}{\kappa}\left(\overline{u'_\iota u'_\iota}^f_k-\frac{2}{3}\kappa\right)-\varepsilon \tag{24}$$

$$\overline{u'_\iota w'}^f_k=2\nu_{tk}\bar{S}_{iz}{}^f_k,\quad C_1=1.8 \tag{25}$$

$$\nu_{tk}=\frac{c_\mu k_k^f}{\varepsilon},k_k^f=\frac{1}{2}\overline{u'_\iota u'_\iota}^f_k\ \ \varepsilon=\frac{1}{\kappa y_p}\left(\frac{k_k^f}{3.3}\right)^{\frac{3}{2}} \tag{26}$$

3 EXPERIMENTAL AND CALCULATION CONDITION OF LOCAL SCOURING AND DEPOSITION AROUND A CYLINDER

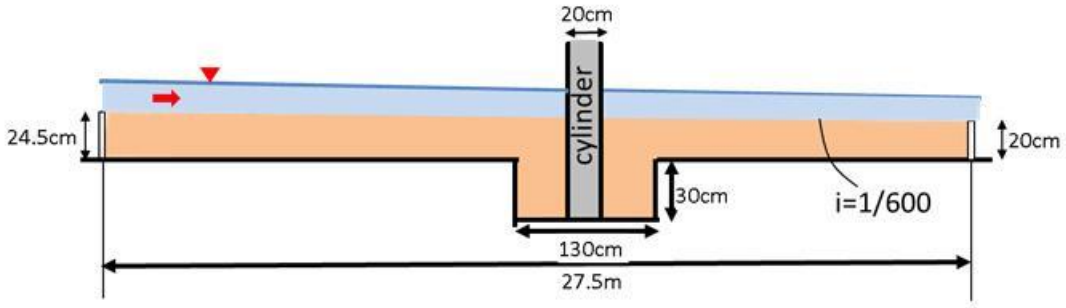

Figure 3. Longitudinal view of the experimental channel (Fukuoka et.al., 1997).

3.1 Experimental conditions

Table 1. Experimental condition.

Channel width	1.5 m	Mean water depth	0.137 m
Channel length	27.5 m	Mean velocity	0.442 m/s
Cylinder diameter	0.2 m	Sediment diameter	0.8 mm
Discharge	90 ℓ/s	Specific gravity	2.59
Initial bed slope	1/600	Sediment supply	0.84 ℓ/min

The calculation model was applied to the experiment on the bed variation around the cylinder in order to clarify the validity of the model. Figure 3 shows a longitudinal view of the movable bed experiment channel (Fukuoka et.al. ,1997). In this experiment, the horizontal and vertical distribution of the flow velocity around the cylinder, the bed variation and the fluid forces acting on the cylinder were measured. Table 1 shows the specifications of the experimental channel and the hydraulic quantity of the experiment. The channel length was 27.5m, the channel width was 1.5m, and the initial bed slope was 1/600. The cylinder was 20cm in diameter and was located at a position of 10.5m from the downstream end of the channel. The particle size of the bed material was 0.8 mm. The discharge from the upstream end was 90 ℓ /s. And, the sediment supply was carried out from the upstream end of the channel.

3.2 Calculation condition

The size of the calculation mesh was 2.5cm square. The initial bed gradient was 1/600 as same as the experimental conditions. After the experiment, the channel beds were lowered by around 2 to 3cm. The initial bed elevations in 5 meshes from the downstream end were lowered by 3cm in order to taking into account of the bed degradations in the experimental results. The uniform bed material of 0.8mm was set. The discharge and sediment volume were given as shown in Table1. The dimension length y_p of the dissipation rate shown in Eq. [26] was set to $1.5\delta_b$ so that the mean water depth and mean flow velocity of the calculation result almost agreed with the experimental results shown in Table 1.

4 CALCULATION RESULTS

Figure 4 shows the experimental and calculation results of the flow velocity distribution at a height of 0.07m below the water surface. The calculation results almost explained experimental results of the flow velocity upstream of the cylinder and the range of separation area downstream of the cylinder. Figure 5 compares the velocity at near the bed of the experiment results with the calculated velocity on surface of the transition layer. Although the calculation results could explain the range of the reverse flow at near the beds in front of the cylinder, the calculated range of the separation in the lee of the cylinder was wider than the measured one

Figure 6(a) indicates the bed variation contour of the experimental results. And Figure 6(b) and Figure 6(c) show the calculation results of bed variation and the velocity vector in the bed load layer. The bed load layer thicknesses of the calculations were set in 2 and 5 times the particle size, respectively. Figure 6(d) indicates the calculation result of the bed surface velocity vector and bed variation by the conventional sediment transport model in Japan. The conventional model was conducted by using the equilibrium sediment discharge formula (Ashida, et.al, 1972) and sediment entrainment formula (Itakura, et.al, 1984). Those

calculation results were compared with the experiment, after the bed scouring in front of the cylinder became almost stable which was 20 minutes after start of the calculation. The developed model explained that the channel bed was scoured from the front of the cylinder toward the rear, although the scour depth in the front of the cylinder was larger than the experimental results (see Figure 6(a), Figure 6(b) and Figure 6(c)). The conventional model shown in Figure 6(d) explained the scouring in front of the cylinder, but could not reproduce the scouring of the rear of the cylinder.

On the other hand, the developed calculation model could not explain range of the sediment deposition in the downstream of the cylinder. This was because the separation area behind the cylinder and its velocity distribution were not to be properly calculated.

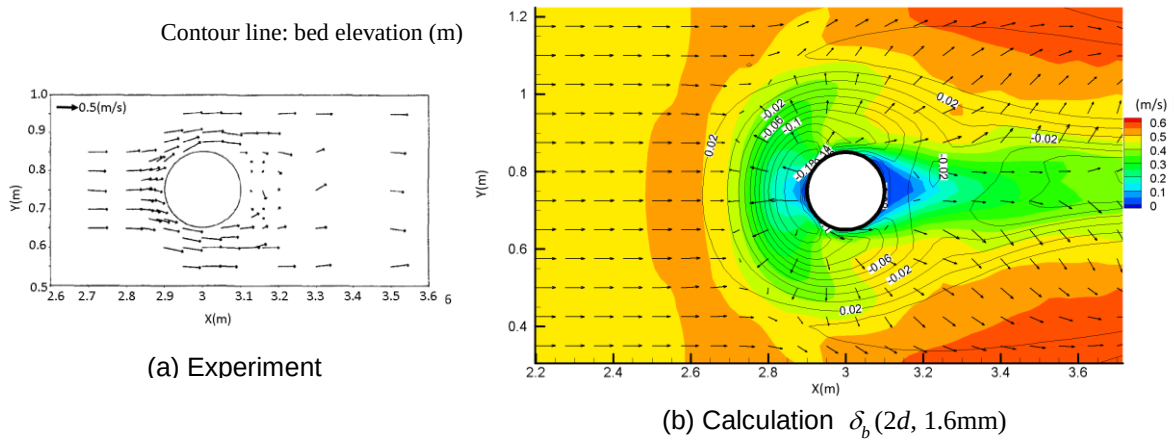

(a) Experiment

(b) Calculation $\delta_b\,(2d,\ 1.6\mathrm{mm})$

Figure 4. Horizontal velocity distribution at a height of 0.07m below the water surface.

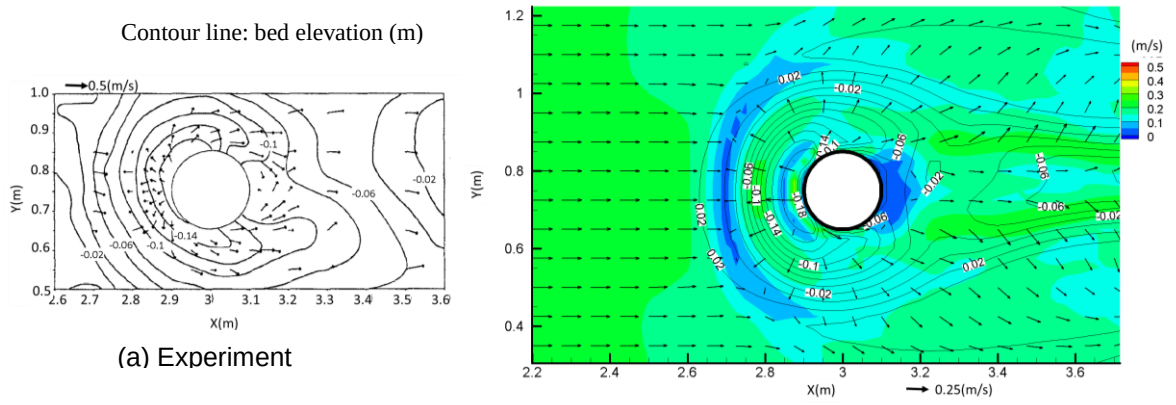

(a) Experiment

(b) Calculation $\delta_b\,(2d,\ 1.6\mathrm{mm})$

Figure 5. The experimental velocity distribution near the beds and the calculated surface velocity of the transition layer.

Figure 7 indicates the contour diagrams of the vertical component of turbulence intensities in the bed load layer. The bed load thicknesses were 2 and 5 times the sediment particle size, respectively. Figure 8 shows the contour diagrams of the sediment entrainment amounts and flow velocity in the bed load layer. The calculation results indicated that the turbulence intensities increased and sediment entrainments occurred in front and side of the cylinder. And the sediments movements occurred in the rear of the cylinder shown in Figure 9. Figure 9 shows calculation results of particle velocities of the bed load layer and the contour lines of the bed elevations of the in the case that the bed load layer thickness was twice the particle size. The developed model was able to explain the bed scouring around the cylinder by calculating those non-equilibrium flows and sediment movements near the beds.

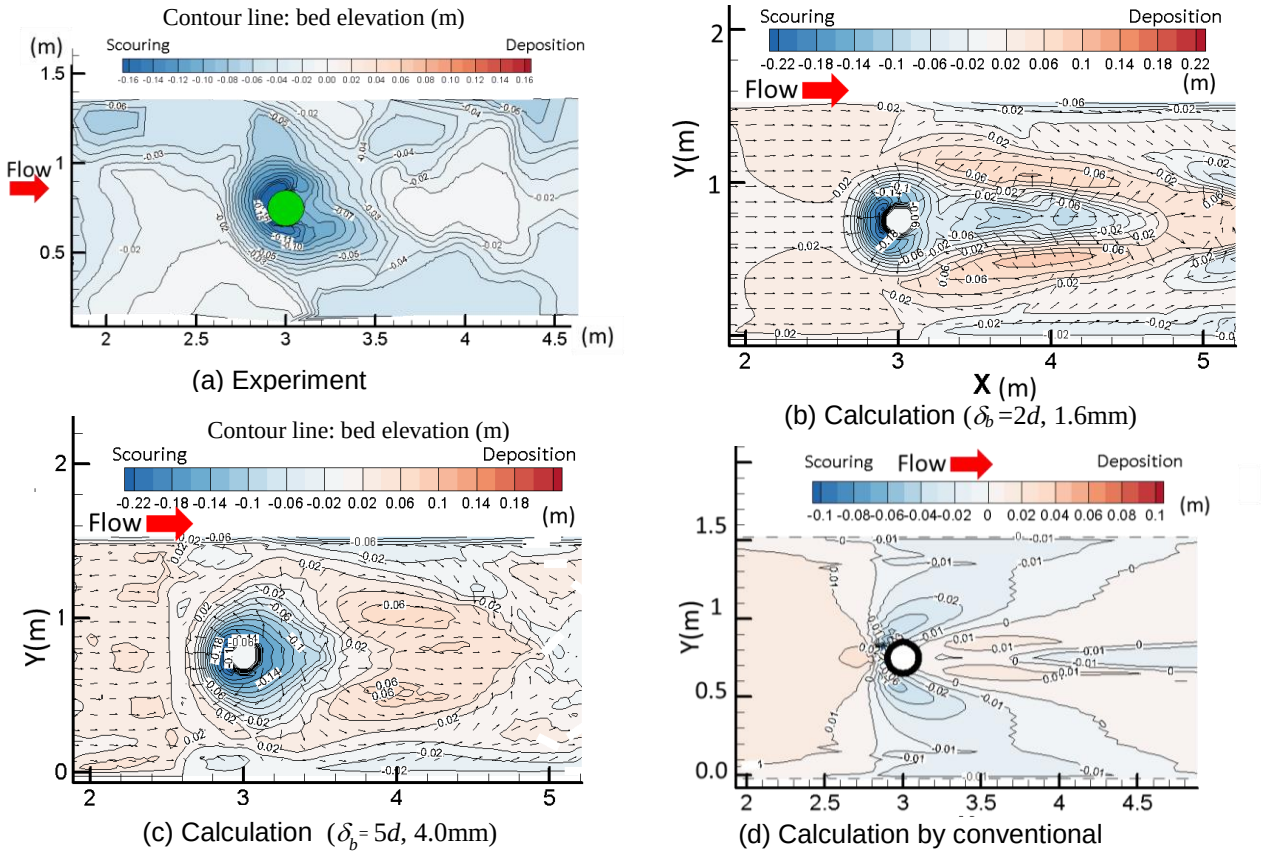

Figure 6. The contour of the bed variations in the experiment and calculation by the developed model (δ_b=2d, δ_b=5d) and the conventional model.

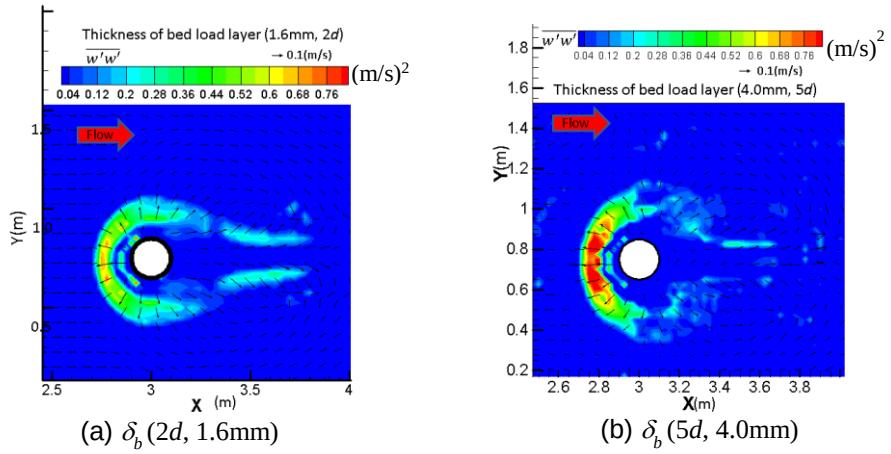

Figure 7. The turbulence intensity in the bed load layer.

The differences of bed variations by the thickness of bed load layer introduced are shown in Figure 6(b) and Figure 6(c). The bed scouring in the thick bed load layer became deeper than that of the thin bed load layer. And, the turbulence intensity in the bed load layer was also larger than that of the thin bed load layer (see Figure 7). Figure 10 shows a longitudinal sectional view of the calculated velocity distributions. The bed load thicknesses were 2 and 5 times the sediment particle size, respectively. And the flow velocity distributions were shown along the center line of the channel. The range and intensity of reverse flow in front of the cylinder having the thick bed load layer was larger than those having thin bed load layer. Those results suggest that the calculation model should consider the changes in the thickness of the bed load layer associated with non-equilibrium flows and sediment transports near the beds.

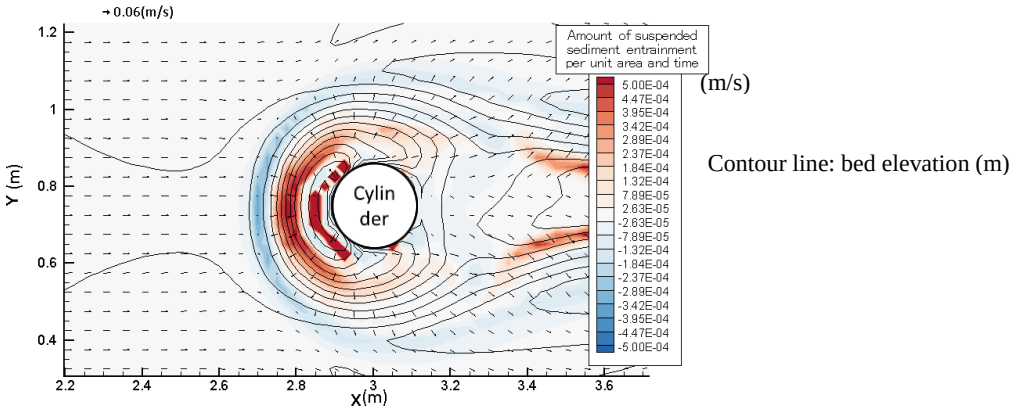

Figure 8. The amount of the suspended sediment entrainment. (δ_b =2d, 1.6mm)

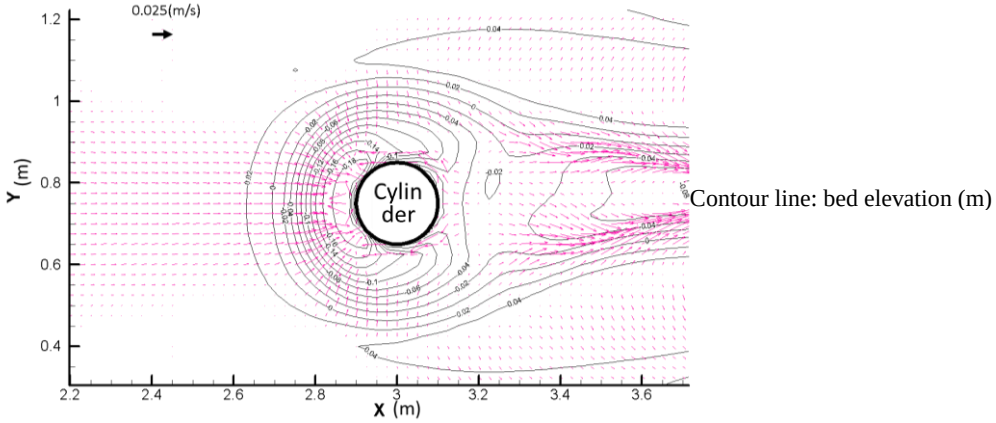

Figure 9. The velocity vector of sediment particle in the bed load layer. (δ_b =2d, 1.6mm)

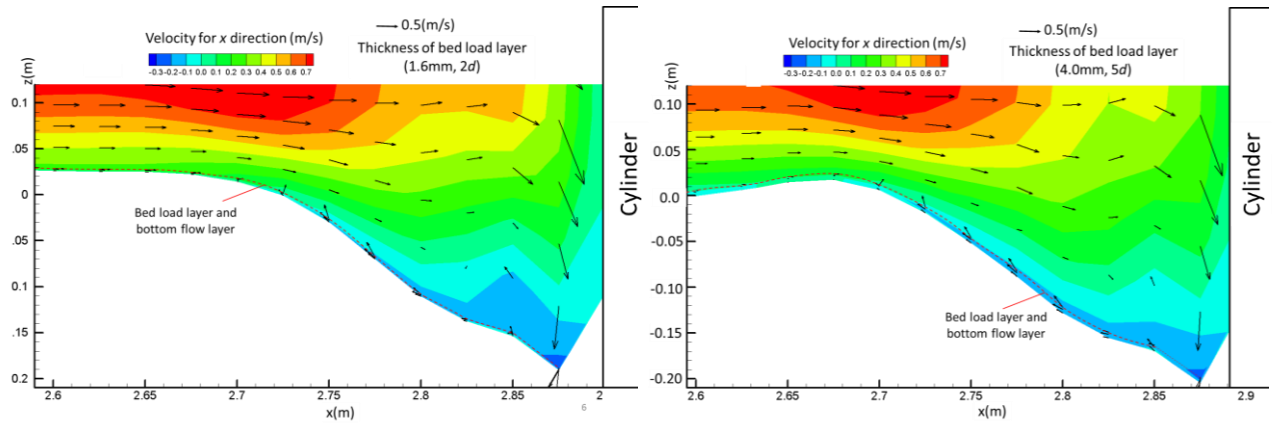

(a) δ_b (2d, 1.6mm) (b) δ_b (5d, 4.0mm)

Figure 10. The longitudinal and vertical velocity distribution of flow in front of the cylinder.

5 CONCLUSIONS

The quasi-3D flood flow and bed variation calculation model was developed by considering non-equilibrium two-phase motion of flows and sediments near beds. The calculation model was able to explain the bed scouring in front and side of the cylinder.

However, the calculation model was not able to elucidate the range and scale of the sediment depositions downstream of the cylinder because the separating flow from the cylinder was inaccurately calculated. In additions, the differences in thickness of the bed load layer introduced in the model affected degrees of flow and bed variation around the cylinder. It is required to be improved so that the thickness of bed load layer should vary with flows and sediment transports in the bed load layer.

REFERENCES

Ashida, K. and Michiue, M. (1972). Study on Hydraulic Resistance and Bed-Load Transport Rate in Alluvial Streams, *Proceedings of JSCE*, JSCE, Vol.206, pp.59-69.

Chauchat, J., Cheng, Z., Nagel, T., Bonamy, C. and Hsu, T.J. (2017). SedFoam-2.0: a 3-D Two-Phase Flow Numerical Model for Sediment Transport, *Geoscientific Model Development*, Vol.10, Issue12, 4367–4392.

Clift, R., Grace, J.R. and Weber, M.E. (1978). Bubbles,Drops and Particles, *Academic Press*.

Fukuoka, S., Miyagawa, T. and Tobiishi, M. (1997). Measurements of Flow and Bed Geometry around a Cylindrical Pier and Calculation of its Fluid Forces. *Proceedings of Hydraulic Engineering*, Vol.41, 729-734.

Itakura, T. and Kishi, T. (1980). Open Channel Flow with Suspended Sediments. *Journal of the Hydraulic Division*, ASCE, HY8, 1325-1343.

Lane, E. W. and Kalinske, A. A. (1941). Engineering Calculations of Suspended Sediments. *Transactions, American Geophysical Union*, Vol.22, pp. 603-607.

Leo C. van Rijn. (1984). Sediment Transport, Part I: Bed Load Transport. *Journal of Hydraulic Engineering*, Vol.110, Issue10.

Nakagawa, H., Tsujimoto, T., Murakami, S. and Gotoh, H. (1990). Transition Mechanism from Saltation to Suspension in Bed-Material-Load Transport. *J. Hydrosci. and Hydraul. Eng*, 8(1), 41-54.

McLean,S.R., Nelson, J.M., Wolfe, S.R. (1994). Turbulence Structure over Two-Dimensional Bed Forms: Implications for Sediment Transport. *Journal of Geophysical Research*, Vol.99, No.C6, 12, 729-747.

Shugar, H. D., Kostaschuk, R., Best, L. J., Parsons, R. D., Lane, N. S., Orfeo, O., and Hardy, J. R. (2010). On the Relationship between Flow and Suspended Sediment Transport over the Crest of a Sand Dune, Rı´o Parana´, Argentina. *International Association of Sedimentologists, Sedimentology*, 57, 252–272.

Uchida, T. and Fukuoka, S. (2014). Numerical Calculation for Bed Variation in Compound-Meandering Channel Using Depth Integrated Model without Assumption of Shallow Water Flow, *Advances in Water Resources*, Vol.72, 45-56.